Experimental and Theoretical Investigation of the Phase Behavior of Naproxen in Supercritical CO_2[†]

Michael Türk*

Institut für Technische Thermodynamik and Kältetechnik, Universität Karlsruhe (TH), Engler-Bunte-Ring 21, D-76131 Karlsruhe

Thomas Kraska

Institut für Physikalische Chemie der Universität zu Köln, Luxemburger Str. 116, D-50939 Köln

New experimental solubility data of Naproxen in supercritical CO_2 for (313 to 353) K and pressures ranging from (15 to 40) MPa are presented. This covers the range where processes with supercritical fluids such as Rapid Expansion from Supercritical Fluids are typically performed. In addition, the solid−liquid−gas equilibrium line for the CO_2 + Naproxen system was determined from (0.1 to 30) MPa. The solubility data are correlated by three different methods: two methods for the density−solubility correlation and one method for the pressure−solubility correlation. Different literature data and predictions of the sublimation pressure of Naproxen, which are required for the solubility correlation, are compared.

Introduction/State of the Art

Most pharmaceutical compounds are administered to the human body in a solid dosage form (approximately 80 %) or by injection. If the dissolution behavior of a drug is poor, a high dosage is needed and hence may cause some side effects to the human body. A large number of publications show that a promising method for enhancement of the dissolution rate of poor water-soluble drugs in the biological environment is the reduction of the particle size. Today, several conventional micronization techniques have been utilized for particle size reduction. These micronization techniques include milling and grinding, spray-drying, freeze-drying, high-pressure homogenization, and ball and air jet milling. The disadvantages of these techniques are degradation of the product, a broad particle size distribution, and cumbersome solids handling.[1−4] To overcome this, supercritical fluid based particle size reduction processes are gaining in importance in material science and pharmaceutical technology since they are characterized by various advantages such as low temperature and a solvent-free product. The primary techniques are: rapid expansion of supercritical solutions (RESS), particle generation from gas saturated solution (PGSS), and gas antisolvent (GAS) and its numerous modifications. Solubility data are essential for an accurate experimental design and for calculation of the concentration of supercritical solutions at different operating conditions. In the case of the RESS process, an insufficient solubility limits the practical applicability. Moreover, the phase behavior, especially the solid−liquid−gas equilibrium line (SLG-line) of the systems involved, has to be known. RESS experiments show that the product properties such as particle size, size distribution, and morphology are often strongly influenced by the underlying phase behavior.[5−8]

In this paper, experimental results for the SLG-line of Naproxen under CO_2 pressure and for the solubility of Naproxen in CO_2 are reported. In the literature, experimental solubility data are available for temperatures ranging from (308 to 348) K within the pressure range of (12 to 35) MPa.[9−11] The solubility of *S*-(+)-Naproxen in CO_2 was determined at temperatures of 313 K, 323 K, and 333 K and in the pressure range between (9 and 19) MPa by Ting et al.[9] These authors used a flow technique coupled with gravimetric analysis to measure the solubility of Naproxen in CO_2. Suleiman et al.[11] used a high-pressure chromatographic system equipped with a high-pressure online UV detector and a conventional dynamic solubility apparatus to measure the solubility of racematic Naproxen at 313 K and pressures between (12 and 28) MPa. The authors show that these data are in good agreement with the data published by Ting et al. An integrated supercritical fluid extraction/supercritical fluid chromatography system, equipped with a static system for solubility determination in the supercritical fluid extraction mode, was used by Garmroodi et al.[10] These authors measured solubility data at temperatures (308 K, 318 K, 328 K, 338 K, and 348 K) and pressures, (12.2 to 35.5) MPa, different from those reported by Ting et al. and by Suleiman et al. For the data, published by Garmroodi et al., no information about the enantiomer is given, so one might speculate that they used the racemate. Although each individual set of data follows mostly a common trend, in some cases the published data exhibit different trends with respect to temperature or pressure. Therefore, the solubility of Naproxen in CO_2 was determined here at 313 K, 323 K, 333 K, 343 K, and 353 K and pressures between (15 and 40) MPa. These solubility data were correlated using empirical density-based models and a method based on an accurate noncubic equation of state for the solvent CO_2 which allows also the correlation of the solubility as a function of the pressure.[12,13]

Experimental

Materials and Methods. Naproxen (CAS 22204-53-1) is an odorless, white crystalline substance and member of the

* Corresponding author. Tel.: + 49 (0)721 608 2330. Fax: + 49 (0) 721 608 2335. E-mail: mt@ttk.uni-karlsruhe.de.

[†] Part of the "Gerhard M. Schneider Festschrift".

10.1021/je800920d CCC: $40.75
Published on Web 02/24/2009

Table 1. Physical Properties of Pure CO_2[17] and of Pure Naproxen

substance	M / g·mol^{-1}	T_C / K	p_C / MPa	ρ_C / kg·m^{-3}	T_{fus}[a] / K	$\Delta_{fus}h$[a] / kJ·mol^{-1}	$p_{2,sub}$[b] / Pa	$p_{2,sub}$[c] / Pa	$V_{2,m}$[d] / cm^3·mol^{-1}
CO_2	44.01	304.1	7.38	467.6	–	–			
Naproxen	230.3				427.7	31.4	$6.89 \cdot 10^{-5}$	$3.34 \cdot 10^{-3}$	178.3

[a] Measured with DSC. [b] At 313 K, calculated from:[18] $\log(p/\text{Pa}) = 17.2655 - 6706.556/(T/\text{K})$. [c] At 313 K, calculated from:[19] $\log(p/\text{Pa}) = 15.2781 - 5558.775/(T/\text{K})$. [d] Ting et al.[9]

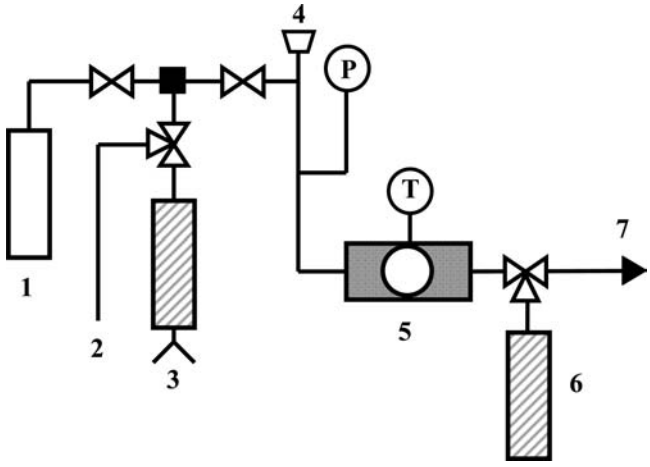

Figure 1. Schematic diagram of the phase behavior apparatus: 1, gas cylinder; 2, vacuum connection; 3, manual piston pump; 4, pressure-relief valve; 5, high-pressure view cell; 6, catchment tank; 7, outlet; P, pressure indicator; T, temperature indicator.

arylacetic acid group of nonsteroidal anti-inflammatory drugs. The use of Naproxen is suggested for the treatment of rheumatoid arthritis and is also indicated in the relief of mild to moderate pain. *S*-(+)-Naproxen ((*S*)-(+)-6-methoxy-α-methyl-2-naphthalene acetic acid) was supplied by Sigma-Aldrich Chemie GmbH, Taufkirchen (Germany).

Differential scanning calorimetry (DSC) was used for physical characterization (melting temperature and enthalpy of fusion) of Naproxen. A DSC 204 Phoenix (Netzsch; Germany) was used to perform the measurements. The sample (≈5 mg per run) was heated in an aluminum standard pan under a nitrogen gas flow of 20 mL·min^{-1}. Usually, a heating rate of 5 K·min^{-1} was used up to a maximum temperature of 473 K.

CO_2 (Air Liquid, Germany; purity greater than 99.99 %) was chosen as the supercritical solvent since it is a nonflammable, inexpensive, and nontoxic solvent. Due to the low critical temperature, supercritical CO_2 allows processing at moderate temperatures.

All materials and solvents were of the purest grade available and were used without additional purification. In Table 1, some important physical properties of the materials used in this study are summarized.

SLG-Line. A schematic diagram of the apparatus used for the determination of the SLG-line and solubility of Naproxen in CO_2 is shown in Figure 1. A variable heatable high-pressure cell ($V = (3.3 \text{ to } 7.3)$ cm^3), equipped with two sapphire windows ($D = 8$ mm), was used to conduct the melting point depression study of Naproxen. In the case of the solubility measurements, the pressure vessel is equipped with an internal magnetic stir bar.

In a typical experiment, an excess of the solid solute (ca. 0.1 g) was loaded into the high-pressure equilibrium cell, and CO_2 was gradually introduced into the view cell. The SLG-line of Naproxen under CO_2 pressure was determined either by finding the melting temperature at a constant pressure or finding the melting pressure at a constant temperature. Repeated measurements (usually 3-fold) were performed to minimize the influence of kinetic effects on the onset of melting. More details about the experimental procedure are given in the literature.[14,15]

Table 2. Experimental Pressure−Temperature Data of the SLG-Line for the CO_2 + Naproxen System

T/K	p/MPa
413.6	30.0
414.3	25.0
414.5	22.5
415.7	20.0
417.8	15.0
419.7	11.4
420.7	10.0
422.9	7.51
424.1	5.04
424.4	4.97
425.6	2.48
427.7[a]	0.10

[a] Measured with DSC.

Solubility. The solubility of Naproxen in CO_2 was determined using a static method[14−16] coupled with gravimetric analysis described by Sherman et al. in detail.[16] Usually a known amount of solute, (0.02 to 0.04) g, inside a vial was weighed with a precise balance (± 0.1 mg) and loaded into the high-pressure equilibrium cell. Afterward, the vessel was slowly filled with CO_2. Once the desired temperature was reached, the desired pressure was adjusted by the manual piston pump. After sufficient time (usually > 12 h) was allowed for equilibration of the CO_2 + solute solution, the vessel was depressurized and opened, and the vial was reweighed. Hence, the difference between the initial and the final measured mass of solute gave the amount of Naproxen dissolved in CO_2. The amount of CO_2 metered into the cell was determined by weighing the CO_2-cylinder before and after CO_2 had been filled into the cell using a balance (± 0.02 g). The solubility of Naproxen in CO_2, Y_2, can then be calculated from the dissolved amount of Naproxen divided through the mass of CO_2 metered into the cell. Usually, each data point measurement was conducted two times giving a reproducibility ranging from 3 % at high pressure up to 12 % at low pressure due to the small amount of solute dissolved in CO_2 and therewith low solubility.

The temperature in the high-pressure equilibrium cell is measured with a thermocouple, which is calibrated against a Pt-25 thermometer. The accuracy of the temperature measurement was within the total limit of ± 0.2 K. A piezoresistive pressure gauge (class 0.1) was used to measure the system pressure, and the total uncertainty of the pressure measurement was less than 0.05 MPa.

Results and Discussion

Melting-Point Depression. The experimental pressure−temperature data for the SLG-line of the CO_2 + Naproxen system are listed in Table 2 and depicted in Figure 2. The normal melting point of Naproxen at ambient pressure was verified using DSC and was found to be 427.7 K. The enthalpy of fusion

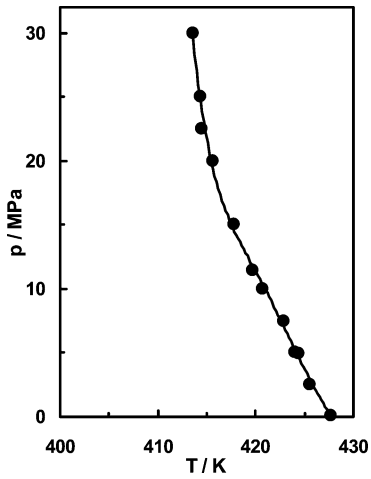

Figure 2. Pressure−temperature trace of the experimental three-phase SLG-line for the CO_2 + Naproxen system: full circles, this work.

Table 3. Solubility of Naproxen (2) in CO_2 (1) Expressed in Terms of Mass of Naproxen per Mass of CO_2 (Y_2) and in Terms of Naproxen Mole Fraction (y_2)[a]

T	$p_{2,sub}$[b]	p	ρ_1			
K	Pa	MPa	mol·dm^{-3}	Y_2	y_2	$E = y_2 \cdot p/p_{2,sub}$
313	$6.89 \cdot 10^{-5}$	15.14	17.775	$8.04 \cdot 10^{-5}$	$1.54 \cdot 10^{-5}$	$3.37 \cdot 10^{+6}$
		19.97	19.082	$1.08 \cdot 10^{-4}$	$2.07 \cdot 10^{-5}$	$6.01 \cdot 10^{+6}$
		25.14	20.002	$1.31 \cdot 10^{-4}$	$2.51 \cdot 10^{-5}$	$9.14 \cdot 10^{+6}$
		29.86	20.659	$1.63 \cdot 10^{-4}$	$3.12 \cdot 10^{-5}$	$1.35 \cdot 10^{+7}$
323	$3.18 \cdot 10^{-4}$	15.11	15.957	$9.06 \cdot 10^{-5}$	$1.73 \cdot 10^{-5}$	$8.23 \cdot 10^{+5}$
		20.13	17.869	$1.52 \cdot 10^{-4}$	$2.90 \cdot 10^{-5}$	$1.84 \cdot 10^{+6}$
		25.41	18.965	$1.90 \cdot 10^{-4}$	$3.59 \cdot 10^{-5}$	$2.87 \cdot 10^{+6}$
		30.01	19.779	$2.16 \cdot 10^{-4}$	$4.13 \cdot 10^{-5}$	$3.90 \cdot 10^{+6}$
		34.95	20.426	$2.07 \cdot 10^{-4}$	$3.95 \cdot 10^{-5}$	$4.34 \cdot 10^{+6}$
		39.60	20.952	$2.38 \cdot 10^{-4}$	$4.54 \cdot 10^{-5}$	$5.66 \cdot 10^{+6}$
333	$1.33 \cdot 10^{-3}$	15.05	13.758	$9.88 \cdot 10^{-5}$	$1.88 \cdot 10^{-5}$	$2.13 \cdot 10^{+5}$
		20.04	16.446	$1.51 \cdot 10^{-4}$	$2.89 \cdot 10^{-5}$	$4.33 \cdot 10^{+5}$
		25.00	17.858	$2.54 \cdot 10^{-4}$	$4.84 \cdot 10^{-5}$	$9.06 \cdot 10^{+5}$
		30.11	18.876	$2.69 \cdot 10^{-4}$	$5.13 \cdot 10^{-5}$	$1.16 \cdot 10^{+6}$
		35.01	19.606	$3.04 \cdot 10^{-4}$	$5.82 \cdot 10^{-5}$	$1.53 \cdot 10^{+6}$
		39.72	20.191	$3.62 \cdot 10^{-4}$	$6.92 \cdot 10^{-5}$	$2.06 \cdot 10^{+6}$
343	$5.16 \cdot 10^{-3}$	15.07	11.568	$8.48 \cdot 10^{-5}$	$1.62 \cdot 10^{-5}$	$4.73 \cdot 10^{+4}$
		20.08	15.016	$1.88 \cdot 10^{-4}$	$3.60 \cdot 10^{-5}$	$1.40 \cdot 10^{+5}$
		24.99	16.746	$3.02 \cdot 10^{-4}$	$5.76 \cdot 10^{-5}$	$2.79 \cdot 10^{+6}$
		29.94	17.893	$3.80 \cdot 10^{-4}$	$7.26 \cdot 10^{-5}$	$4.21 \cdot 10^{+6}$
		34.99	18.772	$4.63 \cdot 10^{-4}$	$8.85 \cdot 10^{-5}$	$6.00 \cdot 10^{+6}$
		39.91	19.461	$5.19 \cdot 10^{-4}$	$9.92 \cdot 10^{-5}$	$7.67 \cdot 10^{+6}$
353	$1.85 \cdot 10^{-2}$	15.16	9.863	$7.86 \cdot 10^{-5}$	$1.50 \cdot 10^{-5}$	$1.23 \cdot 10^{+4}$
		20.04	13.514	$2.53 \cdot 10^{-4}$	$4.84 \cdot 10^{-5}$	$5.25 \cdot 10^{+4}$
		25.03	15.598	$5.20 \cdot 10^{-4}$	$9.90 \cdot 10^{-5}$	$1.34 \cdot 10^{+5}$
		28.82	16.664	$6.08 \cdot 10^{-4}$	$1.16 \cdot 10^{-4}$	$1.81 \cdot 10^{+5}$
		34.61	17.859	$7.49 \cdot 10^{-4}$	$1.43 \cdot 10^{-4}$	$2.68 \cdot 10^{+5}$
		39.62	18.648	$9.65 \cdot 10^{-4}$	$1.84 \cdot 10^{-4}$	$3.95 \cdot 10^{+5}$

[a] The CO_2-density is taken from NIST Chemistry WebBook.[17] [b] Calculated from:[18] $\log(p/\text{Pa}) = 17.2655 - 6706.556/(T/\text{K})$.

(31.4 kJ·mol^{-1}) obtained from DSC analysis is in excellent agreement with the value (31.5 kJ·mol^{-1}) published by Perlovich et al.[18] For the CO_2 + Naproxen system, the $\Delta p/\Delta T$ slope of the SLG-line is negative in the pressure range investigated. The melting temperature decreased from the normal melting point continuously to 413.6 K at 30 MPa. Thus, a solid−fluid two-phase equilibrium (s_2 = g) exists for pressures equal to or below 30 MPa and temperatures from (305 to 413) K.

Experimental Solubility Data. In Table 3, the solubility of Naproxen in CO_2 is expressed in terms of mass of Naproxen per mass of supercritical CO_2 (Y_2) and in terms of Naproxen mole fraction (y_2). At 313 K, Y_2 increases from $8 \cdot 10^{-5}$ at 15 MPa to $1.6 \cdot 10^{-4}$ at 29.9 MPa and from $7.9 \cdot 10^{-5}$ at 15.2 MPa to $9.7 \cdot 10^{-4}$ at 39.6 MPa and 353 K. The comparison with the

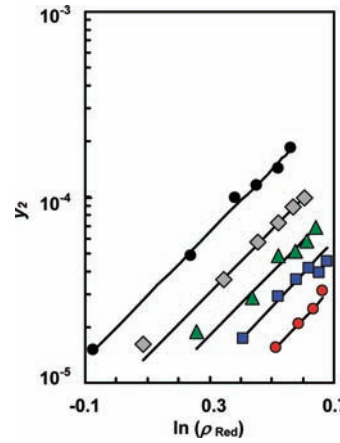

Figure 3. Solubility of Naproxen in CO_2 at different temperatures: red circles, 313 K; squares, 323 K; triangle-up, 333 K; diamond, 343 K; full circles, 353 K; solid lines are calculated with eq 2.

data published by Ting et al.[9] at around (15 and 20) MPa shows a very good agreement at 323 K (in each case ≤ 2 %) but larger deviations at 313 K (12 % and 15 %) and 333 K (16 % and 8 %). The crossover pressure for the system CO_2 + Naproxen was found to be around 15 MPa. Above the crossover pressure, the solubility increases with increasing temperature, and below this value, due to the decrease in CO_2-density with increasing temperature, the reverse is the case. In Table 3, the calculated enhancement factor (E) is also included. This factor can be regarded as a normalized solubility because it removes the effect of the sublimation pressure. E is defined as the ratio of the mole fraction of Naproxen over the solubility in an ideal gas

$$E = \frac{y_2 \cdot p}{p_{2,\text{sub}}} \tag{1}$$

In eq 1, E is the enhancement factor and $p_{2,sub}$ is the sublimation pressure of the solute at temperature T. In this work, $p_{2,sub}$ is calculated from eq 1a

$$\log\left(\frac{p_{2,\text{sub}}}{p_0}\right) = A + \frac{B}{(T/\text{K})} \tag{1a}$$

where A and B were fitted to experimental data[18] and $p_0 = 1$ Pa is the unit pressure. It is seen from Table 3 that the enhancement factor varies from $1.2 \cdot 10^4$ to $1.3 \cdot 10^7$. For comparison, we applied the Watson correlation for solids, as described in Lyman et al.,[19] too. This approach leads to a sublimation pressure which is about 2 orders of magnitude higher than the experimental data (see Table 1) and considerable lower enhancement factors. Both the enhancement factor and the solubility are strongly influenced by the system temperature and the solvents density. The influences of these two variables are shown in Figure 3 which shows the solubility of Naproxen as a function of reduced CO_2-density. The experimental results show trends which are similar to those observed for other solids in the supercritical region. At constant temperature, the logarithm of the solubility of a solute increases almost linearly with the solvent density and therewith solvent power. Figure 3 also shows the pronounced temperature effect on solubility in the region outside the retrograde region. In this region, the effect of the temperature on the solute sublimation pressure overlays the

Table 4. Results of the Empirical Correlation (Equation 2)

T/K	data points	a	b	100·ARD[a]
313	3	−13.2181	4.1513	2.1
323	4	−12.6066	4.0819	2.1
333	5	−12.0990	3.9123	5.5
343	5	−11.5699	3.9152	1.4
353	6	−10.8210	3.9163	4.1
average		−	−	3.2

[a] ARD = $(1/N)\ \sum_1^N (|y_{calc} - y_{exp}|)/(y_{exp})$.

effect of the solvent density, resulting in an increase of the Naproxen solubility with increasing temperature.

Correlation of Experimental Solubility Data. The reliable experimental determination of solubility in SCFs and its accurate correlation is important for the development of supercritical fluid technology. Until today, models based on equations of state, together with different mixing rules, are the most widely used ones to correlate and predict the solubility in SCFs. Recently, the importance of the accurate knowledge of the required thermophysical data, such as critical parameters, acentric factor, solid molar volume, and sublimation pressure of the solutes, has been demonstrated by Burgos-Solórzano et al.[20] and by Coimbra et al.[21] Moreover, the estimation methods for pharmaceutical compounds, polymers, biomolecules, and other complex molecules are mostly empirical and often lead to inconsistent and unreliable results. Thus, due to the lack of information on these data, empirical density-based models are often used for the correlation of experimental solubility data.

One of the most commonly used models, which correlates the solubility of a solute in a SCF to the fluids density, has been proposed by Stahl et al.[22] and by Kumar and Johnston[23]

$$\ln(y_2) = a + b\cdot\ln(\rho_{Red}) \quad \text{with} \quad \rho_{Red} = \frac{\rho_1}{\rho_{1,c}} \qquad (2)$$

where subscripts 1 and 2 refer, respectively, to the pure solvent and to the pure solute. In eq 2, y_2 is the mole fraction of Naproxen in CO_2; ρ_1 is the density of CO_2 at the equilibrium temperature T and pressure p; $\rho_{1,C}$ is the critical density of CO_2; and a and b are two empirical constants. To confirm the reliability of the experimental data, we examined the consistency of solubility data using eq 2, and the values obtained for a and b are summarized in Table 4 along with the average relative deviation (ARD). The lines depicted in Figure 3 are calculated with eq 2 and demonstrate that there is a good correlation between calculation values and the experimental data. As can be seen from the ARD, the experimental data are satisfactorily correlated with this empirical correlation with an overall ARD of 3.2 %.

Mendez-Santiago and Teja[24] have shown that eq 3 can be used to calculate the solubility of numerous solids in CO_2. Since the constants A and B are independent of temperature, the solubility data for binary systems at different temperatures should collapse to a single straight line when plotted in terms of $T\cdot\ln E$ vs the CO_2-density. The lower limit of this linear behavior is about half, while the upper limit is around 2-fold of the critical density of the solvent.[24]

$$T\cdot\ln(E) = A + B\cdot\rho_1 \quad \text{with} \quad E = \frac{y_2 p}{p_{2,sub}} \qquad (3)$$

Table 5. Results of the Empirical Correlation (Equation 3)

data points	A	B	100·ARD[a]
25	1811.29[b]	153.2697[b]	2.0
25	923.09[c]	140.4084[c]	−

[a] ARD = $(1/N)\ \sum_1^N (|y_{calc} - y_{exp}|)/(y_{exp})$. [b] Enhancement factor data were calculated with experimental sublimation pressure data.[18] [c] Enhancement factor data were calculated with sublimation pressure data estimated from the Watson correlation.[19]

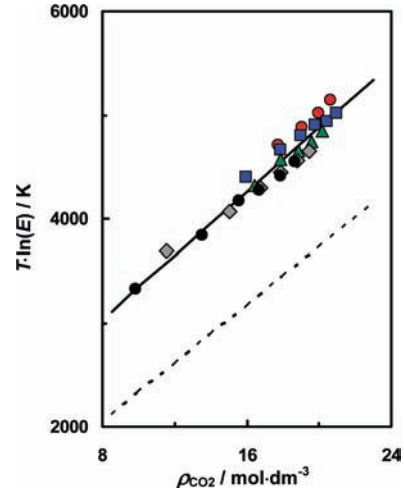

Figure 4. $T\cdot\ln E$ vs solvent density for the CO_2 + Naproxen system: red circles, 313 K; squares, 323 K; triangle-up, 333 K; diamond, 343 K; full circles, 353 K; full line is calculated with experimental sublimation pressure of Perlovich et al.,[18] and dotted line is calculated with the sublimation pressure obtained from the Watson correlation.[19]

The fact that all isotherms collapse to a single line allows determining the self-consistency of experimental data and allows identifying data sets that are not consistent with other data. The constants of eq 3 for the solubility of the CO_2 + Naproxen system are reported in Table 5. The solid line depicted in Figure 4 is the fit over a temperature range of (313 to 353) K. As can be seen in this figure, all isotherms collapse to a single line so that the experimental data are satisfactorily correlated with eq 3 with an overall ARD of 2.0 %. For comparison, we fitted eq 3 to the enhancement factor data calculated with the sublimation pressure which was estimated with the Watson correlation. The resulting constants A and B are listed in Table 5 too, and the corresponding fit is depicted as the dotted line. This curve shows a significant deviation ranging from −22 % to −32 % which is the result of the noticeably higher values from the estimated sublimation pressure data (see also Table 1).

In addition to empirical correlation approaches, we have employed an equation of state method for the correlation of the Naproxen solubility. This method is based on an accurate noncubic equation of state for the supercritical solvent CO_2[25] and a fugacity approach. While one can only correlate the solubility as a function of the density with eq 2 and eq 3, one also can correlate the solubility as a function of the pressure with an equation of state approach. Within this approach, the properties of the solute enter by the sublimation pressure and the molar volume while the solvent enters by its fugacity as

$$y_2 = \frac{p_{2,sub}}{p\cdot\varphi(y_2)} \exp\left(\frac{V_{2,m}(p - p_{2,sub})}{RT}\right) \qquad (4)$$

The fugacity is calculated from the equation of state. Details on the equation of state[25] and the application of the fugacity

approach[12,13] to this equation are given in the literature. The critical parameters of the pure solute do not need to be estimated by a group contribution method because we fit the attraction and covolume equation of state parameter for the solute during the solubility correlation. For the same reason, also no k_{ij} parameter is required. The total number of parameters, fitted in this work, are four, namely, two equation of state parameters of the pure solute and two parameters for the sublimation pressure. As a fitting algorithm, we use a Marquardt−Levenberg method. In cases where the initial parameter values for the correlation are not good enough to get convergence, a Monte Carlo method for generating initial values is employed. Here we focus on the influence of the sublimation pressure on the solubility correlation. The experimental determination of the sublimation pressure of low volatile organic substances is difficult.[26] Often the sublimation pressure is unknown and has to be estimated by empirical methods such as group contribution methods.[19,27] Since the sublimation pressure is required in the correlation of the solubility, one can treat it as an adjustable parameter when fitting the model to solubility data. If solubility data are available for different temperatures, one can build in a Clausius−Clapeyron-like temperature dependence of the sublimation pressure on the temperature

$$p_{2,\mathrm{sub}} = p_0 \exp\left(-\frac{A_{\mathrm{sat}}}{T} + B_{\mathrm{sat}}\right) \tag{5}$$

Here A_{sat} and B_{sat} are adjustable parameters, and $p_0 = 1$ MPa is the unit pressure. The suitability of this approach has been demonstrated for various low volatile substances ranging from dyes in CO_2[12,28] and N_2O[29] to biomolecules.[13] The sublimation pressure obtained in this way from the solubility agrees well with experimental data where available and behaves systematically.[12] Also, the other parameters of the complete model such as the attraction parameter of the solute or its covolume behave systematically in a homologous series of substances such as the anthraquinone dyes for variable length of the alkyl side chains.[28] Here we apply this correlation method in different ways: (A) we correlate eq 5 to the available experimental data of the sublimation pressure;[18] (B) we fit eq 5 to the literature data which are estimated with a group contribution method;[19] and (C) we treat the sublimation pressure as an adjustable property fitting the parameters of eq 5 during the solubility correlation. The value of the molar volume solute is fixed in all correlations to 178.3 $cm^3 \cdot mol^{-1}$, while the compressibility of the solute is set to zero. Hence, only the remaining four parameters are fitted to the data. The resulting values are: for fit (A) $a = 883.735$ K, $b = 81.2094$ $cm^3 \cdot mol^{-1}$, $A_{\mathrm{sat}} = 15442.4$ K, $B_{\mathrm{sat}} = 25.9397$, for fit (B) $a = 829.308$ K, $b = 59.8514$ $cm^3 \cdot mol^{-1}$, $A_{\mathrm{sat}} = 12795.3$ K, $B_{\mathrm{sat}} = 21.3611$, and for fit (C) $a = 805.23$ K, $b = 53.4022$ $cm^3 \cdot mol^{-1}$, $A_{\mathrm{sat}} = 11048.6$ K, $B_{\mathrm{sat}} = 17.2568$. The resulting correlations of the solubility are plotted in Figure 5. The ARD varies around 10 % being higher for the 313 K data. One can see that for (323 to 353) K all correlation methods give similar, reasonable agreement with the experimental data, while for 313 K all correlations give too low solubility. For 323 K, the experimental data are better described if the sublimation pressure is adjusted during the correlation of the solubility (solid curve, $p_{\mathrm{sub,C}}$). The sublimation pressure estimated from a group contribution method[19] gives a lower solubility. If the sublimation pressure is used as an adjustable parameter in the solubility correlation, one obtains a higher sublimation pressure than the values estimated from a group contribution method and from the experimental sublimation pressure data.[18] Especially if one fits the sublimation pressure only to the solubility data for 313 K one obtains a much higher value compared to the experimental data which is due to the general difference between the model and the data at 313 K. Here one can speculate whether the model does not capture the temperature dependence correctly or the experiment gives too high solubility at 313 K. For correlations using the experimental data for the sublimation pressure,[18] the solubility isotherms have a too high curvature. This is due to the small variation of the sublimation pressure over the given temperature range because to reproduce the temperature dependence of the solubility isotherms the model has to vary its parameters during the correlation. So the weak temperature dependence of the sublimation pressure does not agree with the temperature dependence of the solubility. Actually, the group contribution method[19] is reasonably consistent with the solubility data, while the experimental data[18] show less agreement. The reason for this remains unclear. A possible explanation might be related to the purity of the samples used in the literature. For Ibuprofen, which is also a chiral molecule, it is known that the solubility in CO_2 is quite different for the enantiomers and the racemate. This is related to the phase behavior of Ibuprofen. The racemate forms a compound which can be seen in the solid−liquid phase diagram showing a compound at $x = 0.5$ with a higher melting temperature than the enantiomers.[30] For Naproxen, there is no racematic compound, and the two enantiomers rather behave as a eutectic system having a melting point of the racemate a few Kelvin below the melting temperatures of the two enantiomers.[31−33] Still there is an influence of the composition which also shows up in the solubility.

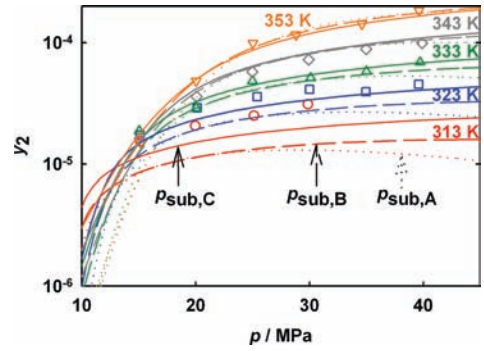

Figure 5. Pressure−mole fraction correlation of the Naproxen solubility using different data for the sublimation pressure. Dotted curves ($p_{\mathrm{sub,A}}$), experimental sublimation pressure of Perlovich et al.;[18] dashed curves, ($p_{\mathrm{sub,B}}$); solid curves ($p_{\mathrm{sub,C}}$), sublimation pressure fitted to solubility data. Symbols are the experimental data: circles, 313 K; squares, 323 K; triangle-up, 333 K; diamond, 343 K; triangle-down, 353 K.

Conclusions

We report new experimental data for the solubility of *S*-(+)-Naproxen in supercritical CO_2 and for the SLG three-phase curve. The solubility data are correlated with three different methods, namely, two easy applicable empirical correlation methods for the solubility−density correlation and an equation of state based method for the solubility−pressure correlation. The correlation methods exhibit good agreement with the data with the exception of the solubility isotherm at the lowest temperature. Both correlation methods can be applied if the used sublimation pressure varies. The agreement with the correlation does not change to a large extent, but the parameters of the model change during the fitting. It turns out that the equation of state based method is more sensitive to the chosen values of the sublimation pressure.

Acknowledgment

The authors thank Mrs. Marlene Crone for conducting the phase behavior measurements.

Literature Cited

(1) Phillips, E. M.; Stella, V. J. Review Article: Rapid expansion from supercritical solutions: application to pharmaceutical processes. *Int. J. Pharm.* **1993**, *94*, l–10.
(2) Perrut, M.; Jung, J.; Leboeuf, F. Enhancement of dissolution rate of poorly-soluble active ingredients by supercritical fluid processes, Part I: Micronization of neat particles, Part II: Preparation of composite particles. *Int. J. Pharm.* **2005**, *288* (3−10), 11–16.
(3) Mishima, K. Biodegradable particle formation for drug and gene delivery using supercritical fluid and dense gas. *Adv. Drug Delivery Rev.* **2008**, *60*, 411–432.
(4) Martín, A.; Cocero, M. J. Micronization processes with supercritical fluids: Fundamentals and mechanisms. *Adv. Drug Delivery Rev.* **2008**, *60*, 339–350.
(5) Diefenbacher, A.; Türk, M. Phase equilibria of organic solid solutes and supercritical fluids with respect to the RESS process. *J. Supercrit. Fluids* **2002**, *22*, 175–184.
(6) Türk, M.; Diefenbacher, A.; Upper, G. *Supercritical Fluids as Solvents and Reaction Media*; Brunner, G., Ed.; Elsevier: Amsterdam, 2004; 147−162.
(7) Blasig, A.; Shi, Ch.; Enick, R. M.; Thies, M. C. Effect of Concentration and Degree of Saturation on RESS of a CO_2-Soluble Fluoropolymer. *Ind. Eng. Chem. Res.* **2002**, *41*, 4976–4983.
(8) Charoenchaitrakool, M.; Dehghani, F.; Foster, N. R.; Chan, H. K. Micronisation by Rapid expansion of Supercritical Solutions to Enhance the Dissolution Rates of Poorly Water-Soluble Pharmaceuticals. *Ind. Eng. Chem. Res.* **2000**, *39*, 4794–4802.
(9) Ting, S. S. T.; Macnaughton, S. J.; Tomasko, D. L.; Foster, N. R. Solubility of Naproxen in Supercritical Carbon Dioxide with and without Cosolvents. *Ing. Eng. Chem. Res.* **1993**, *32*, 1471–1481.
(10) Garmroodi, A.; Hassan, J.; Yamini, Y. Solubilities of the Drugs Benzocaine, Metronidazole Benzoate, and Naproxen in Supercritical Carbon Dioxide. *J. Chem. Eng. Data* **2004**, *49*, 709–712.
(11) Suleiman, D.; Estevez, L. A.; Pulido, J. C.; Garcia, J. E.; Mojica, C. Solubility of Anti-Inflammatory, Anti-Cancer, and Anti-HIV Drugs in Supercritical Carbon Dioxide. *J. Chem. Eng. Data* **2005**, *50*, 1234–1241.
(12) Kraska, T.; Leonhard, K.; Tuma, D.; Schneider, G. M. Solubility of low-volatile solid organic compounds in near- and supercritical fluids. Part II: applications to disperse red 60 and two disubstituted antraquinones. *Fluid Phase Equilib.* **2002**, *194−197*, 471–484.
(13) Kraska, T.; Leonhard, K.; Tuma, D.; Schneider, G. M. Correlation of the solubility of low-volatile organic compounds in near- and supercritical fluids Part I: Applications to natural adamantane and β-carotene. *J. Supercrit. Fluids* **2002**, *23*, 209–224.
(14) Türk, M.; Upper, G.; Hils, P. Formation of composite drug−polymer particles by Co-precipitation during the Rapid Expansion of Supercritical Fluids. *J. Supercrit. Fluids* **2006**, *39*, 253–263.
(15) Türk, M.; Lietzow, R. Formation and stabilization of submicron particles via rapid expansion processes. *J. Supercrit. Fluids* **2008**, *45*, 346–355.
(16) Sherman, G.; Shenoy, S.; Weiss, R. A.; Erkey, C. A Static Method Coupled with Gravimetric Analysis for the Determination of Solubilities of Solids in Supercritical Carbon Dioxide. *Ind. Eng. Chem. Res.* **2000**, *39*, 846–848.
(17) http://webbook.nist.gov/chemistry/fluid/.
(18) Perlovich, G. L.; Kurkov, S. V.; Kinchin, A. N.; Bauer-Brandl, A. Thermodynamics of solutions III: comparison of the salvation of (+)-Naproxen with other NSAIDs. *Eur. J. Pharm. Biopharm.* **2004**, *57*, 411–420.
(19) Lyman, W. J.; Reehl, W. F.; Rosenblatt, D. H. *Handbook of Chemical Property Estimation Methods*; McGraw-Hill: NY, 1982.
(20) Burgos-Solórzano, G. I.; Brennecke, J. F.; Stadtherr, M. A. Solubility measurements and modelling of molecules of biological and pharmaceutical interest with supercritical CO_2. *Fluid Phase Equilib.* **2004**, *220*, 57–69.
(21) Coimbra, P.; Duarte, C. M. M.; de Sousa, H. C. Cubic equation-of-state correlation of the solubility of some anti-inflammatory drugs in supercritical carbon dioxide. *Fluid Phase Equilib.* **2006**, *239*, 188–199.
(22) Stahl, E.; Schilz, W.; Schütz, E.; Willing, E. A Quick Method for the Microanalytical Evaluation of the Dissolving Power of Supercritical Gases. *Angew. Chem., Int. Ed. Engl.* **1978**, *17*, 731–738.
(23) Kumar, S. K.; Johnston, J. P. Modelling the solubility of solids in supercritical fluids with density as independent variable. *J. Supercrit. Fluids* **1988**, *1*, 15–22.
(24) Mendez-Santiago, J.; Teja, A. S. The Solubility of Solids in Supercritical Fluids. *Fluid Phase Equilib.* **1999**, *158−160*, 501–510.
(25) Leonhard, K.; Kraska, T. An equation of state describing the critical region: extension to high pressure. *J. Supercrit. Fluids* **1999**, *16*, 1–10.
(26) Monte, M. J. S.; Santos, L. M. N. B. F.; Fulem, M.; Fonseca, J. M. S.; Sousa, C. A. D. New Static Apparatus and Vapor Pressure of Reference Materials: Naphthalene, Benzoic Acid, Benzophenone, and Ferrocene. *J. Chem. Eng. Data* **2006**, *51*, 757–766.
(27) Reid, R. C.; Prausnitz, J. M.; Poling, B. E. *The Properties of Gases and Liquids*; McGraw-Hill: NY, 1987.
(28) Kraska, T.; Jurtzik, J.; Tuma, D.; Schneider, G. M. Correlation of the solubility of low-volatile organic compounds in near- and supercritical fluids Part III: Application to the antraquinone dye AQ18. *Russ. J. Phys. Chem.* **2003**, *77* (1), 51–57.
(29) Kraska, T.; Tuma, D. High-pressure phase equilibria in binary and ternary mixtures with one near- or supercritical and one high-molecular component. New insights for application and theory. *J. Mater. Sci.* **2006**, *41*, 1547–1556.
(30) Dwivedi, S. K.; Sattari, S.; Jamali, F.; Mitchell, A. G. Ibuprofen racemate and enantiomers: Phase diagram, solubility and thermodynamic studies. *Int. J. Pharm.* **1992**, *87*, 95–104.
(31) Piccolo, O.; Spreafico, F.; Visentin, G.; Valoti, E. Zinc salt catalyzed rearrangement of acetals of optically active aryl 1-chloroethyl ketones: synthesis of optically active 2-arylpropionic acids and esters. *J. Org. Chem.* **1987**, *52*, 10–14.
(32) Giordano, C.; Castaldi, G.; Casagrande, F.; Abis, L. Silver assisted rearrangement of primary and secondary α-bromo-alkylarylketones. *Tetrahedron Lett.* **1982**, *23*, 1385–1386.
(33) Tsuchihashi, G. Synthesis of optically active 2-arylalkanoic acids by the use of 1,2-rearrangement of the aryl group. *Tetrahedron Lett.* **1982**, *23*, 5427–5430.

Received for review November 28, 2008. Accepted February 11, 2009. This work was supported primarily by the Deutsche Forschungsgemeinschaft (DFG, Tu 93/6-1, 6-2, Kr 1598/24-1) which the authors gratefully acknowledge.

JE800920D